Journal of Applied Electrochemistry (2005) 35:297–303
DOI 10.1007/s10800-004-7273-6

Electrochemical removal of hydrogen sulfide from polluted brines using porous flow through electrodes

B.G. ATEYA*, F.M. Al-KHARAFI, R.M. ABDALLAH and A. S. Al-AZAB
*Department of Chemistry, Faculty of Science, Kuwait University, Kuwait P.O. Box 5969 Safat, 13060 Kuwait (*author for correspondence, e-mail: ateya @kuc01.kuniv.edu.kw)*

Received 29 July 2004; accepted in revised form 16 November 2004

Key words: electrochemical oxidation, hydrogen sulfide, porous electrodes, sulfur, flow

Abstract

Carbon felt was used in porous electrodes to achieve electrochemical oxidation of sulfide ions from flowing chloride brines. Using X-ray photoelectron spectroscopy (XPS) and Energy Dispersive Spectroscopy (EDS), sulfur was identified as the final reaction product under various potentials and temperatures. While some of the resulting sulfur flows out with the electrolyte, the rest remains adsorbed on the graphite surface. The rate of the process and the removal efficiency increase with potential, temperature, flow rate and sulfide concentration. The measured limiting currents are substantially lower than those predicted from mass transfer correlations. This was attributed to the passivating effects of the sulfur deposited on the internal surface of the porous electrode. Potentiostatic current transients show that the carbon felt electrodes have higher capacity for removing sulfide ions than planar electrodes, which is attributed to the large internal surface area of the carbon felt.

1. Introduction

Hydrogen sulfide is a dangerous pollutant that is toxic to humans [1] and damaging to metallic materials [2]. It contaminates massive volumes of geothermal brines that are encountered in drilling for oil and gas [3]. It also contaminates a large number of waste waters resulting from industries such as tanneries, pulp and paper, and mining. Consequently, efforts have been directed to the development of methods and strategies to detect, control and/or remove sulfide from such media. These include chemical, biological and electrochemical oxidation, adsorption, use of H_2S scavengers particularly in oil and gas fields [3], and a variety of other methods. A relatively recent review cites many of the earlier works [4].

Electrochemical treatment offers an environmentally attractive method to remove the sulfide ions. It involves anodic oxidation of sulfide containing brines to produce less toxic products [5–9]. Anodic oxidation might also be pursued as a means of using H_2S as a fuel in fuel cells [10, 11], obtaining sulfur from sour gas or for the sole purpose of ridding the media of H_2S and its effects. In view of the high reactivity of sulfur and its many possible oxidation states, the reaction products might be polysulfides, elemental sulfur or oxysalts such as thiosulfates and sulfates [12, 13]. The oxidation of the sulfide ions to produce elemental sulfur (that can be collected) serves the purpose of desulfurization of the brines much more than its oxidation to soluble reaction products. If this can be achieved, the method can provide an attractive and environmentally sound strategy for removing sulfide ions from contaminated brines.

The above processes have been tested in a batch mode of operation. Flow-through porous electrodes possess some attractive features for this purpose [14, 15]. They provide high specific surface areas, and can be operated continuously. Furthermore, they separate the reacted from the non reacted electrolytes when the electrode works with a 100% conversion efficiency per pass. This electrode system has been studied in connection with waste water treatment, e.g. for the recovery of metal ions [15–26], the destruction of organic and inorganic wastes [27–30], the removal of dissolved oxygen [31, 32] , the production of polysulfides from white liquor [33, 34], the storage of energy [35] , the formation of hydrogen peroxide [31, 36] and the recovery of bromine [37, 38].

The objective of this paper is to explore the feasibility of achievement of the anodic oxidation of sulfide ions using porous flow through electrodes and to assess the effects of some operating parameters on the rate of the process.

2. Experimental details

Electrodes were prepared form carbon felt obtained from Alfa Aesar. Figure 1A is an SEM image showing the pore structure of the carbon felt electrode. It has a thickness of 6.35 mm, a density of 0.076 g cm^{-3} and a

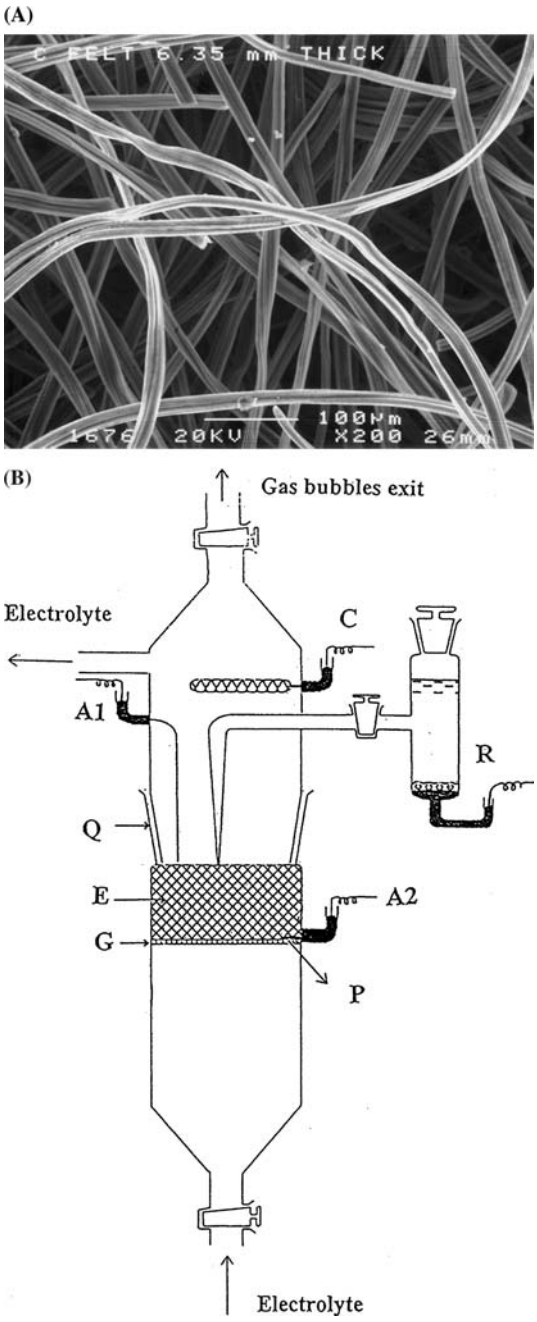

Fig. 1. (A) An SEM image of the carbon felt. (B) A schematic representation of the electrolytic cell. A1 and A2 contacts to the porous electrode (E); C: counter electrode; G: Fritted glass disk; R: reference electrode;Q: ground glass joint; P: platinum connection to the porous electrode.

BET area of 1.61 $m^2\ g^{-1}$. These were characterized by Scanning Electron Microscopy (SEM) (JSM- 6300 JEOL) and BET adsorption using Micromeritics ASAP 2010. The flow through cell was similar to that used previously [15], see Figure 1B. The geometric cross sectional area of the flow through electrode was 5.3 cm^2. The mass of the working electrode amounts to 0.256 g of carbon felt.

The electrolyte was allowed to enter through the bottom (entry) face of the carbon felt electrode and exit through the top (exit) face. The cell was equipped with a platinum wire counter electrode positioned downstream, facing the exit face of the porous electrode. The potential of the exit face of the porous electrode was controlled using a Gamry potentiostat and a saturated calomel reference electrode (SCE). The flow rate of the electrolyte was controlled using a Stepdos 08 RC peristaltic pump obtained from KNF flod's, Germany. Measurements were performed in a supporting electrolyte of 3.5% NaCl. The test solutions were prepared from deionized water and analytical grade chemicals. The temperature of the electrolyte was controlled to ± 1 °C.

3. Results and discussions

3.1. *Electrochemical measurements*

Figure 2 illustrates the potentiodynamic current-potential relations obtained on an electrode operated at a sulfide concentration of 0.1 M at 25 °C and various electrolyte flow rates. The upper part of the curve, at the more noble potentials, describes anodic oxidation while the lower part refers to cathodic reduction. The two parts fall on either side of the open circuit potential. The anodic current increases gradually with potential reaching a well defined limiting value, the magnitude of which increases with the electrolyte flow rate. The limiting current (i_L) is reached at potentials a few hundred mV more noble than the open circuit potential. This indicates that the process is associated with significant levels of electrochemical polarization. The dependence of current on electrolyte flow rate (and on sulfide concentration, as shown below) indicates that the reaction rate is also affected by mass transfer.

The limiting current in a porous flow through electrode depends on the structural properties of the electrode and the transport properties of the electrolyte [15, 18], e.g.,

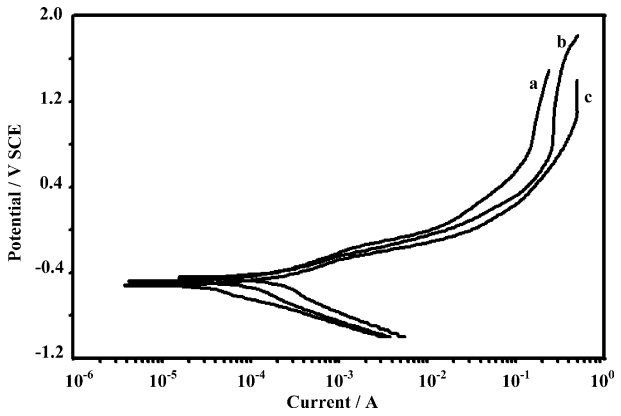

Fig. 2. Effects of the electrolyte flow rate on the current potential relation of the carbon felt electrode: (a) 0, (b) 8 and (c) 80 ml min^{-1}. Electrode thickness is 6.35 mm, sulfide concentration is 0.1 M and voltage scanning rate is 100 mV s^{-1} at 25 °C.

$$i_L = nFQC[1 - \exp(-k_m SLa/Q)] \quad (1)$$

where Q ($cm^3\ s^{-1}$) is the electrolyte flow rate, C is the concentration of the sulfide ions (mol cm^{-4}), k_m is the mass transfer coefficient between the flowing electrolyte and the internal surface of the porous matrix (in cm s^{-1}), S is the specific surface area (area/volume, in cm^{-1}), L is the thickness of the porous electrode and a is its geometric (apparent) cross sectional area (5.3 cm^2). Using the ferricyanide–ferrocyanide couple and the same type of porous electrode, it was found that $k_m S \approx 0.104\ s^{-1}$. Using this value in Equation 1, one calculates limiting currents that are several fold greater than those measured in Figure 2. For example, for $Q = 8$ ml min^{-1} (curve b in Figure 2), the calculated limiting current is 1.39 A while the measured value is only about 250 mA. This discrepancy is attributed to the passivating effects of the resulting sulfur that is deposited on the internal surface of the pores.

The effect of sulfide concentration on the current potential relation is shown in Figure 3 for an electrode operated at a flow rate of 8 ml min^{-1} and a voltage scanning rate of 100 mV s^{-1} at 25 °C. An increase in the concentration increases the current. Figure 4 illustrates the effect of temperature on the current potential relations obtained from an electrode operated at 80 ml min^{-1}, 100 mV s^{-1} and 0.1 M sulfide solution. The increase in temperature has a considerable promoting effect on the current at a certain potential.

Potentiostatic current transients were measured at various potentials, temperatures, sulfide concentrations and electrolyte flow rates. The results are shown in Figure 5A–D, respectively. They indicate that the current depends on the sulfide concentration, electrolyte flow rate, potential and temperature. There is a gradual decrease of current with time. This is attributed to the effects of elemental sulfur which deposits on the internal surface of the porous electrode and tends to passivate it (see below).

Under comparable conditions of potential and sulfide concentrations, the porous electrodes support anodic currents that are much greater than those supported by the graphite electrode, see Figure 6. Furthermore, the current supported by the porous electrode decays with time at a much slower rate than that supported by the nonporous electrode. This indicates that the porous electrode has a higher capacity for removing the sulfide ions than the planar electrode.

The potential distribution within a porous electrode is non uniform. In view of the three dimensional nature of the porous electrodes, there is always a potential shift within the electrode, the magnitude of which depends on the resistivity of the pore electrolyte (ρ), the thickness of the electrode (L) and the distribution of the current produced within the electrode. The potential distribution can only be obtained upon development of a mathematical model of the process and solution of the model equation [23–25]. This is beyond the scope of the present paper. However, an estimate of the maximum possible shift in potential $\Delta E(\max)$ can be obtained assuming the current *(i)* is generated entirely near the bottom face of the porous electrode, i.e.

$$\Delta E(\max) = iL\rho/a \quad (2)$$

Under some conditions [24], about 80% of the current was generated in the top 20% of the thickness of the porous electrode. In such a case the actual potential shift is only about 20% of the value given by Equation 2. The currents at 200 s in Figure 5A–D and 6 amount to 100 mA or less. Using L=0.635 cm, ρ=22 ohm cm and $a = 5.3\ cm^2$, a value of $\Delta E(\max) \approx 270$ mV is obtained. For a current of 10 mA, ΔE(max) amount to only 27 mV. Normally the actual potential drop is much less than $\Delta E(\max)$.

Thus the potential at various locations inside the porous electrode is less noble than the 500 mV (SCE) at the top surface by an amount that ranges from few to 270 mV (as a limiting value). It was shown elsewhere [7] that elemental sulfur formed on solid graphite electrodes at potentials as low as −180 mV (SCE). This indicates

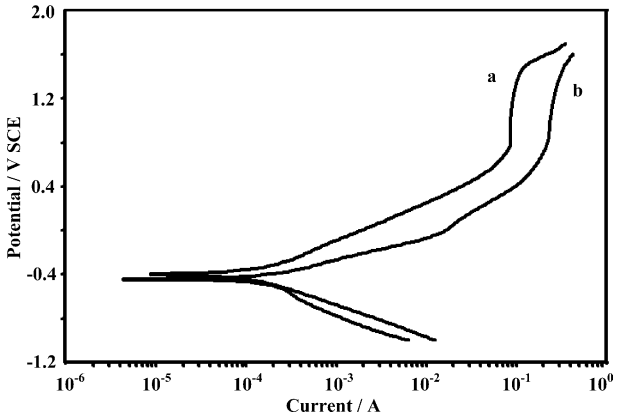

Fig. 3. Effects of sulfide concentration on the current potential relation of the carbon felt electrode at a voltage scanning rate of 100 mV s^{-1}, electrolyte flow rate of 8 ml min^{-1} and 25 °C: (a) 0.01 and (b) 0.1 M sulfide concentration.

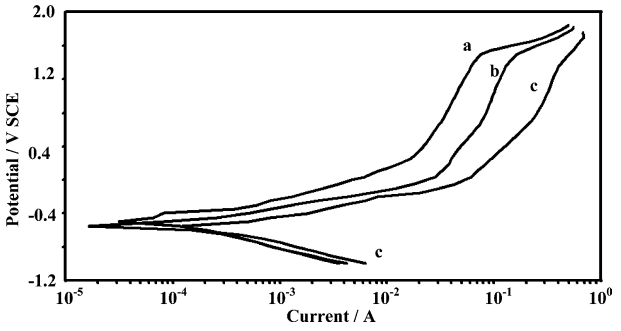

Fig. 4. Effect of temperature on the current potential relation of the carbon felt electrode, at a voltage scanning rate of 100 mV s^{-1}, electrolyte flow rate of 80 ml and sulfide concentration of 0.1 M : (a) 25 °C (b) 50 °C and (c) 80 °C.

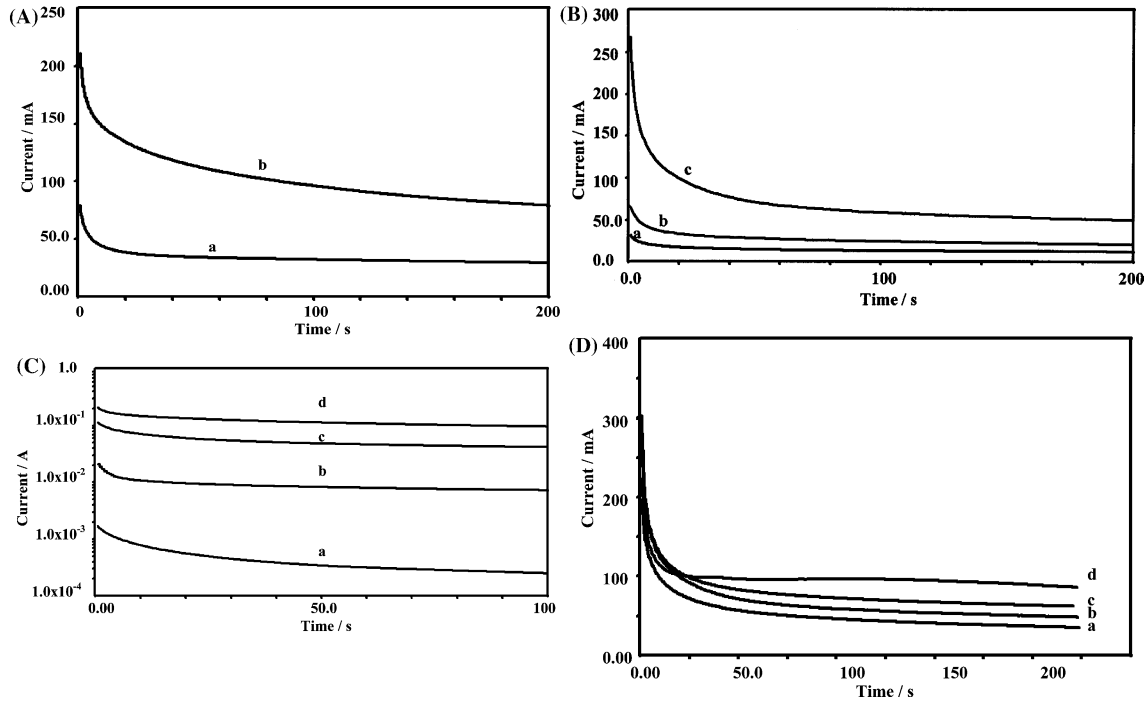

Fig. 5. (A) Current transients supported by the porous flow through electrode, operating on an electrolyte of 0.1 M sulfide and a flow rate of 0 ml/min at 25 °C at different potentials: (a) 0.2 and (b) 0.5 V (SEC). (B) Current transients supported by the porous flow through electrode, operating on an electrolytes of 0.1 M, sulfide at 0.5 V (SEC) at different temperatures: (a) 25 °C (b) 50 °C and (c) 80 °C (C) Current transients supported by the porous flow through electrode, operating on electrolytes of various sulfide concentrations at a potential of 0.5 V (SEC), a temperature of 25 °C and a flow rate of 8 ml min^{-1}: (a) 0.005, (b) 0.01, (c) 0.05 and (d) 0.1 M. (D) Current transients supported by the porous flow through electrode, operating on an electrolytes of 0.1 M sulfide at a potential of 0.5 V (SEC), a temperature of 25 °C and different flow rates: (a) 0, (b) 10, (c) 40 and (d) 80 ml min^{-1}.

that the potential inside the porous electrode is favorable for the formation of elemental sulfur.

The electrochemical behaviour of the sulfide ions in aqueous media is affected by the high reactivity of sulfur and its many oxidation states [12, 13]. Out of the many possible reactions, the following produces elemental sulfur:

$$HS^- = S + H^+ + 2e^- \quad E^\circ = -0.065\,V\ (SHE) \quad (3)$$

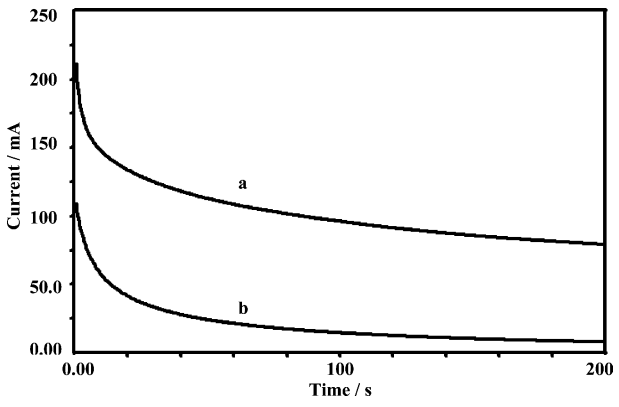

Fig. 6. Comparison of the current transients obtained on : (a) porous flow through electrode and (b) planar graphite electrode at 25 °C and 0.1 M Na_2S at a potential of 0.5 V (SCE).

The resulting atomic sulfur readily polymerizes to give S_8 which is the stable form under ambient conditions. The reaction involves the diffusion of HS^- ions within the pore electrolyte towards the graphite surface. As shown above, the rate of the overall process is affected by diffusion in the electrolyte and by charge transfer across the interface.

3.2. *Characterization of the products*

The formation of elemental sulfur was ascertained in this work using X-ray photo electron spectroscopy (XPS) , Electron Dispersion Spectroscopy (EDS) and SEM. Figure 7 shows a portion of an XPS spectrum of the carbon felt electrode after being polarized at 0.50 V (SCE) for 3 h in the presence of 0.1 M Na_2S at 25 °C. There is a prominent S2p peak at a binding energy of 164.0 eV which compares well with the values of 163.6–164.2 reported for elemental sulfur [39]. The untreated carbon felt did not show this peak. This is a direct proof for the deposition of elemental sulfur on the graphite surface and for its stability under the present experimental conditions. The absence of other prominent peaks suggests that sulfur is the predominant reaction product. Further confirmation of these finding is provided by the results of SEM and EDS measurements on carbon fibers before and after being used for the anodic oxidation of sulfide ions, shown in

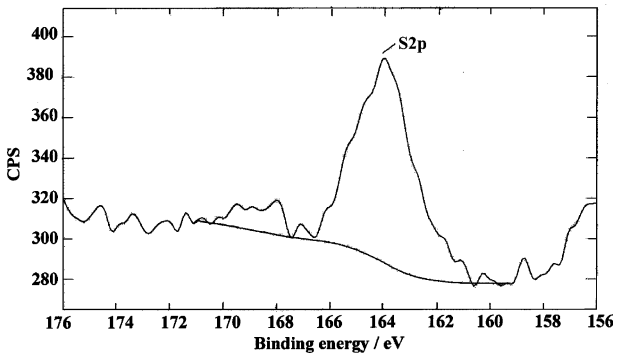

Fig. 7. Portion of the XPS spectrum of the carbon felt electrode polarized for 3 h in a solution containing 0.1 M sulfide at a potential of 0.5 V (SCE) and electrolyte flow rate of 1 ml min^{-1}.

Figure 8 A and B. Note the solid materials that formed on the fibers of the treated electrode (Figure 8B) and the strong sulfur signal at about 2.5 KeV in the EDS spectrum which is ascribed to sulfur. Both features are absent in the SEM image and the EDS spectrum of the untreated fibers (Figure 8A).

Thermodynamic calculations predict that elemental sulfur can, in principle, undergo further oxidation to produce soluble oxyanions [12, 13], e.g.

$$2S + 3H_2O = S_2O_3^{2-} + 6H^+ + 4e^- \qquad E^\circ = 0.465\,V(SHE) \tag{4}$$

$$S + 3H_2O = H_2SO_3 + 4H^+ + 4e^- \qquad E^\circ = 0.449\,V(SHE) \tag{5}$$

$$S + 4H_2O = SO_4^{2-} + 8H^+ + 6e^- \qquad E^\circ = 0.357\,V(SHE) \tag{6}$$

Furthermore, elemental sulfur can also dissolve in the presence of sulfide ions to give several polysulfides [5, 6, 40], e.g.

$$HS^- + xS + OH^- = S_{x+1}^{2-} + H_2O \tag{7}$$

where x=2–5. The fact that elemental sulfur remains stable indicates that the rates of Equations 4–7 are too small compared to the rate of formation of elemental sulfur (Equation 3) under the present conditions of potential and temperature.

3.3. *Removal efficiency*

The amounts of HS^- ions removed in a certain experiment (up to time t) can be calculated from the charge passed, i.e.

$$q(t) = \int_0^t i(t)\mathrm{d}t \tag{8}$$

where $i(t)$ is the current at time t. The value of $q(t)$ can be obtained from graphical integration of the area under each of the curves shown in Figures 5 and 6. These curves reveal that $q(t)$ depends on the electrolyte flow rate, sulfide concentration, potential and temperature. The value of $q(t)$ can be readily converted into "removal efficiency", χ, which has units of moles of HS^- removed per gram of carbon felt. This can be readily achieved using Faraday's law and the mass of the carbon felt electrode, m=0.256 g, i.e.

$$\chi = q(t)/2Fm \quad \text{moles } HS^-/g \text{ carbon felt} \tag{9}$$

where the Faraday constant is F=96484 C mol^{-1}. The factor of 2 in Equation 9 is based on the assumption that reaction 1 is the source of the current with only negligible contributions from reactions 4–6. The XPS results indicate that this is a reasonable assumption in that no other significant peaks are observed. Table 1 lists the values of χ in moles HS^- per gram carbon felt. The results show that the removal efficiency, χ, increases with increase in potential, temperature, concentration and flow rate. Operating for longer time increases χ, as shown in Table 1.

Table 1. Effects of the concentration of sulfide ions, C, electrode potential, E, electrolyte flow rate, Q, temperature, T, and time of electrolysis on the removal efficiency, χ, achieved by carbon felt flow through electrodes, see text

C/M	E/V (SCE)	Q/ml min^{-1}	T/°C	Time/s	χ/mol g^{-1}
0.1	0.2	80	25	200	1.39×10^{-4}
0.1	0.5	80	25	200	4.22×10^{-4}
0.1	0.5	0	25	230	2.35×10^{-4}
0.1	0.5	10	25	230	3.10×10^{-4}
0.1	0.5	40	25	230	3.60×10^{-4}
0.1	0.5	80	25	230	4.45×10^{-4}
0.1	0.5	10	25	200	6.36×10^{-5}
0.1	0.5	10	50	200	1.20×10^{-4}
0.1	0.5	10	80	200	3.10×10^{-4}
0.005	0.5	10	25	100	9.04×10^{-7}
0.01	0.5	10	25	100	1.79×10^{-5}
0.05	0.5	10	25	100	1.08×10^{-4}
0.10	0.5	10	25	100	2.44×10^{-4}

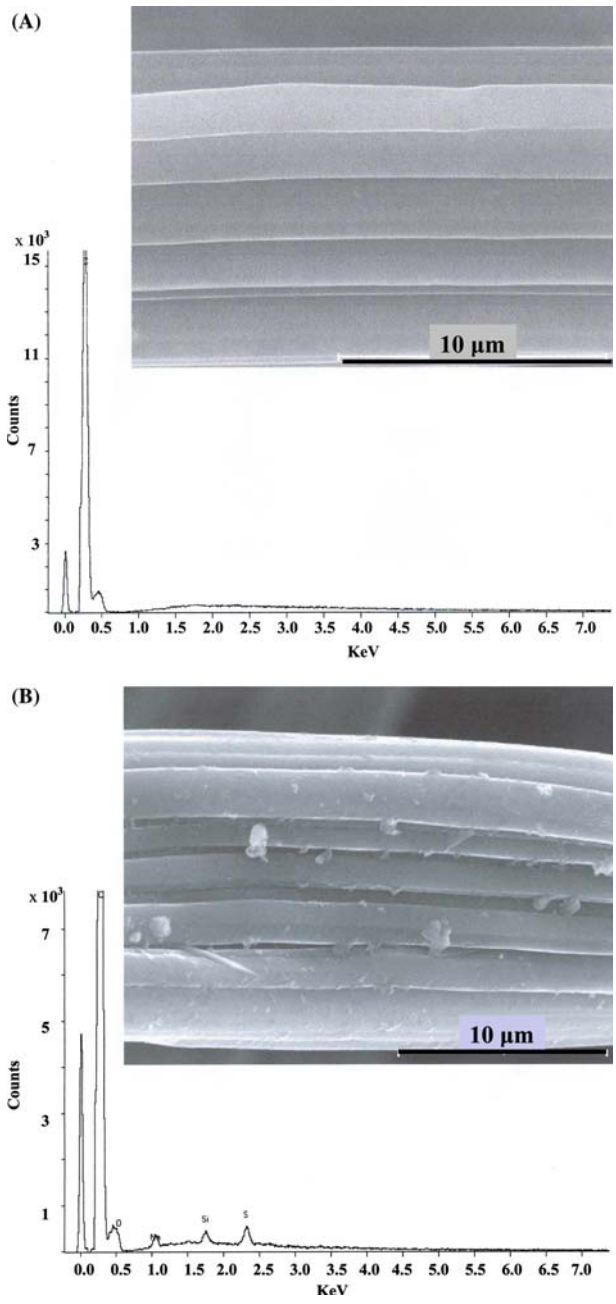

Fig. 8. (A) SEM and EDS of fibers of the carbon felt electrode before it was tested. (B) SEM and EDS of fibers of the carbon felt electrode after it was polarized in a solution containing 0.1 M sulfide at a potential of 0.5 V (SCE) for 3 h.

4. Conclusions

1. Sulfide ions can be directly oxidized to elemental sulfur on carbon felt porous flow through electrodes.
2. The rate of the process is controlled by charge transfer across the interface and by diffusion of the sulfide ions in the pore electrolyte.
3. The carbon felt electrode has a higher capacity than planar electrodes for removing sulfide ions, which is attributed to its large internal surface area.
4. Elemental sulfur remains stable inspite of the thermodynamic calculations that predict its further oxidation to soluble oxyanions and its dissolution to form polysulfides. This indicates that the rates of reactions 4–7 are much smaller than the rate of reaction 1.
5. The reaction rate and hence the removal efficiency increase with sulfide concentration, potential , temperature and electrolyte flow rate.
6. The measured limiting currents are much smaller than those predicted from mass transfer correlations for comparable flow rates. This was attributed to the passivating effects of the sulfur that deposited inside the porous medium. This points to the need to search for methods or strategies to recover sulfur from within the pores so that the electrode can be used again and to search for porous materials that can tolerate high loadings of sulfur without being passivated.

Acknowledgements

The authors are grateful to the Research Administration of Kuwait University for supporting this work, under Grant Number SC04/99, for measurements of the BET area and the usage of the ESCA VG Esca lab 200 under General Facility projects GS01/01 and GS03/01. They also thank the Electron Microscopy unit for performing SEM and EDS measurements.

References

1. ''Extremely Hazardous Substances'' U.S. Environmental Protection Agency, vol. 1 A-L, Noyes Data Corporation, Park Ridge, New Jersey, USA (1988).
2. R.N. Tuttle and R.D. Kane (Ed), 'H_2S Corrosion in Oil and Gas Production', (National Association of Corrosion Engineers, Houston, Texas, 1981).
3. Linda Garverick (Ed.), '*Corrosion in the Petrochemical Industry*' ASM International, Metals Park, Ohio 1994, p. 259.
4. P.N.L. Lens, A. Visser, A.J.H. Janssen, L.W. Hulshoff Pol and G.Lettinga, *Crit. Rev. Environ. Sci. Technol.* **28**(1) (1998) 41.
5. A. Anani, Z. Mao, R.E. White, S. Srinivasan and A.J. Appleby, *J. Electrochem. Soc.* **137** (1990) 2703.
6. A. Anani, Z. Mao, R.E.White, S. Srinivasan and A.J. Appleby, *J. Electrochem. Soc.* **138** (1991) 1299.
7. B.G. Ateya and F.M. Al-Kharafi, *Electrochem. Commun.* **4** (2002) 231.
8. G. Rajalo and T. Petrovskaya, *Environ. Technol.* **17** (1996) 605.
9. N.N. Rao, K.M. Somasekhar, S.N. Kaul and L. Szpyrkowicz, *J. Chem. Tech. Biotech.* **76** (2001) 1124.
10. K. Petrov and S. Srinivasan, *Int. J. Hydrogen Energy*. 21 (1999) 163.
11. J.O'M. Bockris, and U. M. Shahid, Khan, Surface Electrochemistry: A Molecular Level Approach (Plenum Press, London 1993) p. 541, 951.
12. A.J. Bard, R. Parsons and J. Jordan 'Standard Potentials in Aqueous Solutions', (Editor Marcel Dekker, Inc, New York, 1985) p. 94.
13. G.Valensi, J. van Muylder and M. Pourbaix, in M. Pourbaix (Ed.), Atlas of Electrochemical Equilibria in Aqueous Media (NACE, Texas, 1974), p. 545.
14. S.J. Newman, 'Electrochemical Systems', 2nd edn, (Prentice Hall, Engle Wood Cliffs, New Jersey, 1991) p. 487.
15. M.S. Deab, M.M. Saleh, B.E. El-Anadouli and B.G. Ateya, *J. Electrochem. Soc*, **146** (1999) 208.
16. K. Scott and E.M. Paton, *Electrochim. Acta.* **38** (1993) 2191.

17. C. Ponce De Leon and D. Pletcher, *Electrochim. Acta* **41** (1996) 533.
18. D.N. Bennion and J. Newman, *J. Appl. Electrochem.* **2** (1972) 113.
19. V.D. Stankovic and A.A. Wragg, *J. Appl. Electrochem.* **25** (1995) 565.
20. J.M. Bisang, *J. Appl. Electrochem.* **26** (1996) 135.
21. J . van Zee and Newman, *Electrochem. Soc.* **124** (1977) 706.
22. J . Wang and H.M. Dewald, *J. Electrochem. Soc.* **130** (1983) 1814.
23. M.M. Saleh, J.W. Weidner and B.G. Ateya, *J. Electrochem. Soc.* **142** (1995) 4113.
24. M.M. Saleh, J.W. Weidner and B.G. Ateya, *J. Electrochem. Soc.* **142** (1995) 4122.
25. M.M. Saleh, J.W. Weidner and B.G. Ateya, *J. Electrochem. Soc.* **144** (1997) 922.
26. T.L. Hatfield, T.I. Kelven and D.T. Pierce, *J. Appl. Electrochem.* **26** (1996) 567.
27. B.E. Conway, E. Ayranci and H. Al-Maznai, *Electrochim. Acta* **47** (2001) 705.
28. C.S. Hofseth and T.W. Chapman, *J. Electrochem. Soc.* **146** (1999) 199.
29. C. Ponce de Leon and D. Pletcher, *J. Appl. Electrochem.* **25** (1995) 307.
30. P. Cognet, J. Berlan, G. Lacot, P.L. Fabre and J.M. Jud, *J. Appl. Electrochem.* **26** (1996) 631.
31. H. Khalifa, B.G. Ateya and E.A. Arafat, *J. Electroanal. Chem.* **81** (1997) 301.
32. P. Kinzel, H-G. Lintz, P. Gaudebert, V. Bousquet, F. Lapicque and G. Valentin, *J. Appl. Electrochem.* **32** (2002) 951.
33. M. Behm and D. Simonsson, *J. Appl. Electrochem.* **27** (1997) 519.
34. M. Behm and D. Simonsson, *J. Appl. Electrochem.* **29** (1999) 521.
35. P.M. Lessner, F.R. McLarnon, J. Winnick and E. J. Cairns, *J. Appl. Electrochem.* **22** (1992) 927.
36 - A. Huissoud and P. Tissot, *J. Appl. Electrochem*, **29** (1999) 17.
37. Qi. Jian and R.F. Savinell, *J. Appl. Electrochem.* **23** (1993) 873.
38. Qi. Jian and R.F. Savinell, *J. Appl. Electrochem.* **23** (1993) 887.
39. A.R. Gerson and T. Bredow, *Surf. Interface Anal.* **29** (2000) 145.
40. J. Herszage and M. dos S. Afonso, *Langmuir* **19** (2003) 9684.